2013 American Control Conference (ACC)
Washington, DC, USA, June 17-19, 2013

Synchronizing Coupled Semiconductor Lasers under General Coupling Topologies

Shuai Li, Yi Guo, and Yehuda Braiman

***Abstract*— We consider synchronization of coupled semiconductor lasers modeled by coupled Lang and Kobayashi equations. We first analyze decoupled laser stability, and then characterize synchronization conditions of coupled laser dynamics. We rigorously prove that the coupled system locally synchronizes to a limit cycle under the coupling topology of an undirected connected graph with equal in-degrees. Graph and systems theory is used in synchronization analysis. The results not only contribute to analytic understanding of semiconductor lasers, but also advance cooperative control by providing a realworld system of coupled limit-cycle oscillators.**

***Index Terms*— Nonlinear systems, semiconductor lasers, synchronization, coupling topology.**

I. Introduction

Laser diodes (LDs) are compact optical devices that impact large variety of applications including optical communications and optical storage. Despite the advance in laser diode production, the output power from single mode LD remains quite limited. Coherent beam combining provides a viable path to increase coherent emission power from many small lasers. As a consequence of coherent beam combination, in-phase locking of LDs can be realized resulting in a constructive interference along the optical axis. Achieving phase synchronization of LDs poses a very intriguing challenge. Synchronization of semiconductor laser diode array (LDA) comprised of single mode laser diodes has been investigated theoretically predominantly employing the nearest-neighbor and global coupling between the lasers [1]–[4]. General coupling topology has not been explored.

The dynamics of each element of the semiconductor laser array is commonly described by the Lang and Kobayashi equations [5]. In the case of global coupling, the process of synchronization shows analogy to the process found in the Kuramoto model [6]. It is unknown whether this result holds for general coupling topologies of laser arrays. While Kuramoto model describes synchronization behaviors of coupled *phase* oscillators, *coupled laser arrays* have a highly nonlinear model and represent a complex system with both technological [7] and theoretical [8]–[12] importance. From a theoretical perspective, laser arrays provide a prime example of coupled limit-cycle oscillators, which connects to explorations of pattern formation and many other topics throughout physics, chemistry, biology, and engineering [6], [13].

In this paper, we investigate general coupling topologies for coupled semiconductor laser arrays and characterize synchronization conditions. We use graph Laplacian tools inspired by recent cooperative control advances. Examining the dynamic model of coupled semiconductor lasers described by the Lang and Kobayashi equations [5], we first analyze decoupled laser dynamics and reveal local stability properties, and then study coupled laser arrays under general coupling topologies. We characterize synchronization conditions using graph and systems theory. The results not only advance current synchronization methods for semiconductor laser arrays, but also provide a realworld example of coupled high-dimensional nonlinear systems for cooperative control study.

II. The Model of Coupled Semiconductor Lasers

We consider a coupled semiconductor laser system where each laser is subject to the optical feedback reflected from a mirror. Figure 1 shows a globally optical coupled semiconductor array as appeared in [4]. We study the following dynamic equations for n linearly coupled semiconductor lasers [5], [14]–[16]:

$$\begin{aligned}\dot{E}_k &= \frac{1+i\alpha}{2}\left[\frac{g(N_k-N_0)}{1+s|E_k|^2}-\gamma\right]E_k+i\omega E_k \\ &\quad +\frac{K}{m_k}\sum_{j\in\mathcal{N}(k)\bigcup\{k\}}E_j \\ \dot{N}_k &= J-\gamma_n N_k-\frac{g(N_k-N_0)}{1+s|E_k|^2}|E_k|^2 \qquad (1)\end{aligned}$$

where $k=1,\ldots,n$, $\mathcal{N}(k)$ denotes the neighbor set of the kth laser, $m_k=|\mathcal{N}(k)|+1$ with $|\mathcal{N}(k)|$ denoting the number of neighbors of the kth laser, E_k is the complex electric field of laser k and i is the imaginary unit, that is, $\sqrt{-1}=i$. N_k is the carrier number for laser k; ω is the oscillating frequency; $J,\ K>0$ are constant pump current and coupling strength, respectively, both of which are assumed to be identical for all lasers. $\alpha, N_0, s, \gamma, \gamma_n, g$ are system parameters and are

The work was partially supported by the National Science Foundation under Grants EFRI-1024660 and IIS-1218155.

Shuai Li and Yi Guo are with Department of Electrical and Computer Engineering, Stevens Institute of Technology, Hoboken, NJ 07030, USA. {yi.guo,lshuai}@stevens.edu

Yehuda Braiman is with Oak Ridge National Laboratory, Oak Ridge, TN 37831, USA; and also Department of Mechanical, Aerospace, and Biomedical Engineering, University of Tennessee, Knoxville, TN 37996, USA. braimany@ornl.gov

978-1-4799-0178-4/$31.00 ©2013 AACC

all positive, whose physical meaning will be given later in Section V of the paper.

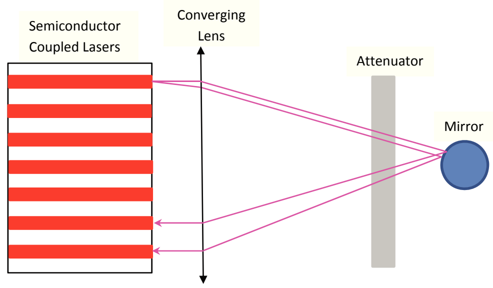

Fig. 1. Schematic representation of a semiconductor coupled laser array with global optical coupling between the lasers [4].

Remark 1: As a special case of all-to-all coupling, the last term in the first equation of (1) becomes $\frac{K}{n}\sum_{j=1}^{n} E_j$, which is consistent with the global coupling model in the literature (*e.g.* [4], [17]).

Remark 2: Figure 1 is an example configuration of globally coupled semiconductor arrays. For different coupling topologies, its physical implementation may be different. To focus on stability analysis utilizing graph Laplacian tools, we do not consider time-delays in our equation, which is practically un-avoidable in some real laser systems (such as external cavity systems [18]). Also, experimental configurations of various coupling topologies are out of the scope of the paper.

We have the following assumption on the coupling topology.

Assumption 1: Assume each laser has the same number of neighboring connections, and the coupling topology between lasers can be described by a general undirected connected graph with a Laplaican matrix L.

The above assumption indicates $|\mathcal{N}(k)| = |\mathcal{N}(j)|$ for any j, k, and $m_i = m_j = m$. Recall that the in-degree (or equivalently out-degree for undirected graphs) is defined to be the number of connections of each node, so that Assumption 1 indicates that each node of the laser network has the same in-degree. We define the Laplician matrix as $L = [L_{ij}]$ with $L_{ij} = -\frac{1}{m}$ for $j \neq i$, $j \in \mathcal{N}(i)$, $L_{ij} = 0$ for $j \neq i$, $j \notin \mathcal{N}(i)$ and $L_{ii} = \frac{m-1}{m}$.

Inspired by the consensus-based work, we re-write the dynamic equation (1) in the following form with a coupling term in the form of relative electrical field:

$$\begin{aligned}
\dot{E}_k &= \left[\frac{1+i\alpha}{2}\left(\frac{g(N_k-N_0)}{1+s|E_k|^2}-\gamma\right)+K\right]E_k + i\omega E_k \\
&\quad + \frac{K}{m}\sum_{j\in\mathcal{N}(k)}(E_j - E_k) \\
\dot{N}_k &= J - \gamma_n N_k - \frac{g(N_k-N_0)}{1+s|E_k|^2}|E_k|^2 \qquad (2)
\end{aligned}$$

To facilitate analysis, we represent the electrical field of each laser as $E_k = r_k e^{i\theta_k} = r_k\cos\theta_k + i r_k \sin\theta_k$ in polar coordinates. We obtain the coupled laser dynamics as

$$\begin{aligned}
\dot{r}_k &= \frac{1}{2}\left(\frac{g(N_k-N_0)}{1+s{r_k}^2}-\gamma+2K\right)r_k \\
&\quad + \frac{K}{m}\sum_{j\in\mathcal{N}(k)}(r_j\cos(\theta_j-\theta_k)-r_k) \\
\dot{\theta}_k &= \frac{\alpha}{2}\left(\frac{g(N_k-N_0)}{1+s{r_k}^2}-\gamma\right)+\omega \\
&\quad + \frac{K}{m}\sum_{j\in\mathcal{N}(k)}\frac{r_j}{r_k}\sin(\theta_j-\theta_k) \\
\dot{N}_k &= J-\gamma_n N_k - \frac{g(N_k-N_0)}{1+s{r_k}^2}{r_k}^2 \qquad (3)
\end{aligned}$$

where $k = 1, \ldots, n$.

Assume identical frequency ω for each laser, we are interested in the synchronization behaviors. We define laser synchronization as the trajectories of all the lasers approaching each other:

Definition 1: The system (1) is said to synchronize if

$$E_k(t) \to E_j(t), \qquad \forall k, j = 1, \ldots, n, \quad as \quad t \to \infty. \qquad (4)$$

The problem of interest is to characterize the conditions so that the system (1) synchronizes.

Note that the above equations describe a three-dimensional dynamic system of coupled lasers with a given oscillating frequency ω. Before investigating dynamics of the coupled laser system, we start in the next section to investigate the stability property of a decoupled laser, that is, the dynamics without the coupling terms in (3).

III. Stability Properties of Decoupled Semiconductor Laser

In this section, we analyze local stability of a decoupled laser, which is described by the equation (3) without the coupling terms. Note that this is also the dynamics of coupled lasers when they're fully synchronized, *i.e.* when $E_1 = E_2 = \ldots = E_n$. We re-write the decoupled laser dynamics as:

$$\begin{aligned}
\dot{r} &= f_r(r,N) = \frac{1}{2}\left(\frac{g(N-N_0)}{1+sr^2}-\gamma+2K\right)r \\
\dot{\theta} &= f_\theta(r,N) = \frac{\alpha}{2}\left(\frac{g(N-N_0)}{1+sr^2}-\gamma\right)+\omega \\
\dot{N} &= f_N(r,N) = J-\gamma_n N - \frac{g(N-N_0)}{1+sr^2}r^2 \qquad (5)
\end{aligned}$$

We notice there exists an equilibrium solution to

$$\begin{aligned}
&\dot{r}^* = \frac{1}{2}\left(\frac{g(N^*-N_0)}{1+sr^{*2}}-\gamma+2K\right)r^* = 0 \\
&\dot{\theta}^* = -\alpha K + \omega \\
&\dot{N}^* = J-\gamma_n N^* - \frac{g(N^*-N_0)}{1+sr^{*2}}r^{*2} = 0 \qquad (6)
\end{aligned}$$

in terms of electrical field with constant amplitude r^* and a constant angular speed ω. The corresponding trajectory of the system is on a circle with $(r, \theta, N) = (r^*, \theta^*, N^*)$, where (r^*, θ^*, N^*) is the nontrivial solution of above equations, which can be computed as:

$$r^* = \sqrt{\frac{gJ - g\gamma_n N_0 - (\gamma - 2K)\gamma_n}{(\gamma - 2K)(\gamma_n s + g)}} \quad (7a)$$

$$\theta^* = (-\alpha K + \omega)t + \theta_0 \quad (7b)$$

$$N^* = \frac{sJ + \gamma - 2K + gN_0}{g + s\gamma_n} \quad (7c)$$

where θ_0 is the initial phase angle.

This solution exists only when the pump current J is larger than a threshold J_{th} given by

$$J_{th} = \gamma_n(N_0 + (\gamma - 2K)/g). \quad (8)$$

To ensure the pump current is positive and the solution to (7a) exists, the coupling strength K must satisfy $K < \gamma/2$.

Since in the dynamic equation (5), the phase variable θ has no influence to the amplitude variable r and the carrier number variable N, we first analyze the stability of the (r, N) system, and then consider the behavior of the θ dynamics. For this purpose, we linearize the decoupled laser system (5) around its equilibrium point $(r, N) = (r^*, N^*)$ to get the linearized form,

$$\begin{aligned} \dot{r} &= \frac{-s\gamma' r^{*2}}{1 + sr^{*2}}(r - r^*) + \frac{gr^*}{2(1 + sr^{*2})}(N - N^*) \\ \dot{N} &= -\frac{2\gamma' r^*}{1 + sr^{*2}}(r - r^*) + (-\gamma_n - \frac{gr^{*2}}{1 + sr^{*2}})(N - N^*) \end{aligned} \quad (9)$$

where $\gamma' = \gamma - 2K$.

Define new states as $\Delta r = r - r^*$, $\Delta N = N - N^*$, the linearized system is re-written as

$$\frac{d}{dt}\begin{bmatrix} \Delta r \\ \Delta N \end{bmatrix} = A \begin{bmatrix} \Delta r \\ \Delta N \end{bmatrix} \quad (10)$$

where

$$\begin{aligned} A &= \begin{bmatrix} \frac{-s\gamma' r^{*2}}{1+sr^{*2}} & \frac{gr^*}{2(1+sr^{*2})} \\ -\frac{2\gamma' r^*}{1+sr^{*2}} & -\gamma_n - \frac{gr^{*2}}{1+sr^{*2}} \end{bmatrix} \\ &\stackrel{def}{=} \begin{bmatrix} A_{11} & A_{12} \\ A_{21} & A_{22} \end{bmatrix} \end{aligned} \quad (11)$$

We can see that the local stability of the system (10) depends on the eigenvalues of the matrix A. The following theorem provides stability results of the decoupled semiconductor laser system (5).

Theorem 1: For the system parameter $0 < K < \gamma/2$, the decoupled semiconductor laser system (5) locally converges to the limit cycle $(r, N) = (r^*, N^*)$ with the angular velocity $\dot{\theta} = (-\alpha K + \omega)$.

Proof: We first analyze the linearized system (10) by solving the equation $|\lambda I - A| = 0$ to find the eigenvalues λ of matrix A. The trajectory of (10) is asymptotically stable if the two eigenvalues of A satisfy $Re\{\lambda_1\}, Re\{\lambda_2\} < 0$.

Since λ_1, λ_2 are the roots of the quadratic equation

$$\lambda^2 + (\gamma_n + \frac{(g + s\gamma')r^{*2}}{1 + sr^{*2}})\lambda + \frac{(g + \gamma_n s)\gamma' r^{*2}}{1 + sr^{*2}} = 0 \quad (12)$$

denoting $a = 1$, b and c as the coefficients of the first order term and the constant, their values can be computed by λ_1, $\lambda_2 = (-b \pm \sqrt{\Delta})/2a$. Whether they are two distinct real roots or two distinct complex roots, depends on the sign of the discriminant $\Delta = b^2 - 4ac$ of above equation. If $b > 0$, $\Delta \geq 0$, the roots are both real. They are negative numbers if and only if $-b + \sqrt{\Delta} < 0$, which implies $b^2 > b^2 - 4ac$. With $a = 1$, we have $0 < c \leq b^2/4$. If $\Delta < 0$, the roots are two distinct complex roots with negative real parts. In this case, we have $c > b^2/4a = b^2/4$. If $b \leq 0$, for any value of Δ, the roots can not both have negative real parts. Following the above statement, the condition for $Re\{\lambda_1\}, Re\{\lambda_2\} < 0$ is $b, c > 0$. For arbitrary positive system parameters $g, s, \alpha, \gamma, \gamma_n, N_0 > 0, J > T_{th}$, together with $r^{*2} > 0$, the condition

$$c = \frac{(g + \gamma_n s)\gamma' r^{*2}}{1 + sr^{*2}} > 0 \quad (13)$$

is satisfied if and only if $\gamma' = \gamma - 2K > 0$, that is $K < \gamma/2$. Moreover, if $\gamma' > 0$, the condition

$$b = \gamma_n + \frac{(g + s\gamma')r^{*2}}{1 + sr^{*2}} > 0 \quad (14)$$

is automatically satisfied. Therefore, if the coupling strength $0 < K < \gamma/2$, the system (10) is asymptotically stable. Using Lyapunov indirect (linearization) method, the nonlinear system (9) is asymptotically stable around (r^*, N^*). That is, $\lim_{t\to\infty} r = r^*$ and $\lim_{t\to\infty} N = N^*$.

Now let's consider the dynamic of θ in equation (5). As the right hand side of this equation is continuous with respect to r and N, we have

$$\begin{aligned} \lim_{r\to r^*, N\to N^*} \dot{\theta} &= \frac{\alpha}{2}(\frac{g(N^* - N_0)}{1 + sr^{*2}} - \gamma) + \omega \\ &= -\alpha K + \omega \end{aligned} \quad (15)$$

Therefore, $\lim_{t\to\infty} \dot{\theta} = -\alpha K + \omega$. This completes the proof. ∎

IV. Synchronization of Coupled Semiconductor Lasers

In this section, we consider n coupled semiconductor lasers described in (3). We can see that the system is a high-dimensional coupled nonlinear system. From the decoupled laser stability analysis in the above section, we know that the limit cycle with a constant angular velocity is the dynamics of coupled lasers when they're fully synchronized. As we are interested in the local synchronization behavior around this equilibrium set, we can linearize the system around the limit cycle with $(r_k, N_k) = (r^*, N^*)$. Note that in synchronization, $\theta_k \to \theta_j, \forall k, j$.

Define new states:

$$\begin{aligned}\Delta r_k &= r_k - r^* \\ \Delta N_k &= N_k - N^* \\ \Delta\theta'_k &= \theta_k - \bar{\theta} = \theta_k - \frac{1}{n}\sum_{i=1}^{n}\theta_i \end{aligned} \tag{16}$$

where r^*, N^* are defined in (7), $\Delta\theta'_k$ measures the difference between the phase of the kth laser and the mean phase of all lasers $\bar{\theta}$. We assume initially the phase differences between lasers are small. Linearizing the system (3) around the equilibria $(r_k, N_k, \Delta\theta'_k) = (r^*, N^*, 0), \forall k$, simplifying using $\sum_{i=1}^{n}\sum_{j\in\mathcal{N}(i)}(\Delta\theta'_j - \Delta\theta'_i) = 0$ due to the symmetry of the coupling topology, the system equations of the error states can be written as

$$\begin{aligned}\Delta\dot{r}_k &= A_{11}\Delta r_k + A_{12}\Delta N_k + \frac{K}{m}\sum_{j\in\mathcal{N}(k)}(\Delta r_j - \Delta r_k) \\ \Delta\dot{\theta}'_k &= -B_1(\Delta r_k - \frac{1}{n}\sum_{i=1}^{n}\Delta r_i) \\ &\quad + B_2(\Delta N_k - \frac{1}{n}\sum_{i=1}^{n}\Delta N_i) + \frac{K}{m}\sum_{j\in\mathcal{N}(k)}(\Delta\theta'_j - \Delta\theta'_k) \\ \Delta\dot{N}_k &= A_{21}\Delta r_k + A_{22}\Delta N_k \end{aligned} \tag{17}$$

where $B_1 = \frac{\alpha s\gamma' r^*}{1+sr^{*2}}$, $B_2 = \frac{\alpha g}{2(1+sr^{*2})}$, A_{11}, A_{12}, A_{21} and A_{22} are the scalar elements of matrix A defined in (11).

We can see that the equilibrium of the system (17) indicates synchronization, that is, at the equilibrium point $(\Delta r_k, \Delta\theta'_k, \Delta N_k) = (0,0,0)$, the states of the system (3) tend to $r_k \rightarrow r_j \rightarrow r^*, N_k \rightarrow N_j \rightarrow N^*, \theta_k \rightarrow \theta_j, \forall k, j$. Note that we linearize the coupled dynamics around $(r^*, N^*, \Delta\theta'_k) = (r^*, N^*, 0)$ as defined in (16), instead of following the convention of usual treatment by linearizing around (r^*, N^*, θ^*). This is because that the linearized model around(r^*, N^*, θ^*) always has a zero eigenvalue in its system matrix, which makes it difficult to analyze local stability. As shown later in this section, we draw local synchronization conclusions by the current treatment.

In matrix form, we have the following compact form,

$$\begin{aligned}\Delta\dot{r} &= A_{11}\Delta r + A_{12}\Delta N - KL\Delta r \\ \Delta\dot{\theta}' &= -B_1 L_0\Delta r + B_2 L_0 \Delta N - KL\Delta\theta' \\ \Delta\dot{N} &= A_{21}\Delta r + A_{22}\Delta N \end{aligned} \tag{18}$$

where $\Delta r = [\Delta r_1, \Delta r_2, ..., \Delta r_n]^T$, $\Delta N = [\Delta N_1, \Delta N_2, ..., \Delta N_n]^T$, $\Delta\theta' = [\Delta\theta'_1, \Delta\theta'_2, ..., \Delta\theta'_n]^T$, $L_0 = I - \frac{\mathbf{1}\mathbf{1}^T}{n}$, L is the Laplacian matrix defined in Assumption 1. For the case with all-to-all coupling, $L = L_0$.

We have the following lemma for the stability of (18).

Lemma 1: The linear coupled system (17) or its compact form (18) is asymptotically stable, if the system parameter $0 < K < \gamma/2$.

Proof: To prove asymptotical stability of (18), we first perform a similarity transformation. Define

$$z = \begin{bmatrix} z_1 \\ z_2 \\ z_3 \end{bmatrix} = M \begin{bmatrix} \Delta r \\ \Delta N \\ \Delta\theta' \end{bmatrix} \tag{19}$$

where

$$M = \begin{bmatrix} P & 0 & 0 \\ 0 & P & 0 \\ 0 & 0 & I \end{bmatrix} \tag{20}$$

where P is the unitary matrix satisfying $PP^T = P^TP = I$ and $PLP^T = \Lambda_0$ with $\Lambda_0 = \text{diag}(\lambda_1, \lambda_2, ..., \lambda_n)$ being the eigenvalue matrix of L, *i.e.*, P is the orthogonal similarity transformation matrix transforming the symmetric matrix L into a diagonal one. With M defined in (20), Eq. (19) can be re-written as,

$$z_1 = P\Delta r \quad z_2 = P\Delta N \quad z_3 = \Delta\theta' \tag{21}$$

Expressing the system (18) in the new coordinates yields,

$$\dot{z}_1 = A_{11}z_1 + A_{12}z_2 - K\Lambda_0 z_1 \tag{22a}$$
$$\dot{z}_2 = A_{21}z_1 + A_{22}z_2 \tag{22b}$$
$$\dot{z}_3 = -B_1L_0P^Tz_1 + B_2L_0P^Tz_2 - KLz_3 \tag{22c}$$

Note that the above equations hold as $A_{11}, A_{12}, A_{21}, A_{22}$ are all scalers. Since $\sum_{k=1}^{n}\Delta\theta'_k = 0$ according to the definitions of $\Delta\theta'_k$ and $\bar{\theta}$, we have $\mathbf{1}^T z_3 = \mathbf{1}^T\Delta\theta' = 0$. Accordingly, $L_0 z_3 = (I - \frac{1}{n}\mathbf{1}\mathbf{1}^T)z_3 = z_3$. Also note that for $c_0 > 0$ we have $LL_0 = LL_0 + c_0\mathbf{1}\mathbf{1}^TL_0 = (L + c_0\mathbf{1}\mathbf{1}^T)L_0$ and $LL_0 = L(I - \frac{1}{n}\mathbf{1}\mathbf{1}^T) = L$. Comparing the right sides of the above two equations, we have $L = (L + c_0\mathbf{1}\mathbf{1}^T)L_0$. Therefore, Eq. (22c) can be re-written as,

$$\begin{aligned}\dot{z}_3 &= -B_1L_0P^Tz_1 + B_2L_0P^Tz_2 - K(L + c_0\mathbf{1}\mathbf{1}^T)L_0z_3 \\ &= -B_1L_0P^Tz_1 + B_2L_0P^Tz_2 - K(L + c_0\mathbf{1}\mathbf{1}^T)z_3 \end{aligned} \tag{23}$$

According to the spectral theorem [19], the eigenvalues of $L + c_0\mathbf{1}\mathbf{1}^T$ are c_0, λ_2, λ_3, $...\lambda_n$ with $\lambda_i > 0, i = 2, \ldots, n$, denoting the ith smallest eigenvalue of L. Replacing (22c) with (23), we can re-write the system dynamics of (22) as follows,

$$\dot{z}_1 = A_{11}z_1 + A_{12}z_2 - K\Lambda_0 z_1 \tag{24a}$$
$$\dot{z}_2 = A_{21}z_1 + A_{22}z_2 \tag{24b}$$
$$\dot{z}_3 = -B_1L_0P^Tz_1 + B_2L_0P^Tz_2 - K(L + c_0\mathbf{1}\mathbf{1}^T)z_3 \tag{24c}$$

The system matrix W of the above linear system is

$$W = \begin{bmatrix} A_{11}I - K\Lambda_0 & A_{12}I & 0 \\ A_{21}I & A_{22}I & 0 \\ -B_1L_0P^T & B_2L_0P^T & -K(L + c_0\mathbf{1}\mathbf{1}^T) \end{bmatrix} \tag{25}$$

To prove that z converges to zero, it is sufficient to prove that the eigenvalues of W locate on LHP. Note that W is a block lower triangular matrix, and the diagonal block $-K(L + c_0\mathbf{1}\mathbf{1}^T)$ has eigenvalues $-Kc_0$, $-K\lambda_2$, $-K\lambda_3$, $...-K\lambda_n$, all of which locate on LHP. Therefore, we only need to prove that the following matrix

$$\left[\begin{array}{cc} A_{11}I - K\Lambda_0 & A_{12}I \\ A_{21}I & A_{22}I \end{array}\right] \tag{26}$$

has all eigenvalues on LHP in order to prove the fact that the eigenvalues of W locate on LHP. In fact, this is equivalent to the asymptotically stability of the following subsystem composed of z_1 and z_2:

$$\begin{array}{rcl} \dot{z}_1 & = & A_{11}z_1 + A_{12}z_2 - K\Lambda_0 z_1 \\ \dot{z}_2 & = & A_{21}z_1 + A_{22}z_2 \end{array} \tag{27}$$

For the system (27), it is clear that this system is composed of n completely decouple subsystems. Therefore, its stability is equivalent to stability of all the subsystems. To show this more clearly, we write (27) into the following scalar form,

$$\begin{array}{rcl} \dot{z}_{1i} & = & A_{11}z_{1i} + A_{12}z_{2i} - K\lambda_i z_{1i} \\ \dot{z}_{2i} & = & A_{21}z_{1i} + A_{22}z_{2i} \end{array} \tag{28}$$

where z_{1i} and z_{2i} are the ith component of the vector z_1 and that of z_2 respectively. The system (27) is asymptotically stable if the following system matrices for all subsystems are Hurwitz,

$$A - K\lambda_i \left[\begin{array}{cc} 1 & 0 \\ 0 & 0 \end{array}\right] --- \text{Hurwitz} \tag{29}$$

The characteristic polynomial for the above matrix is:

$$\begin{array}{c} \lambda^2 + (\gamma_n + \frac{(g+s\gamma')r^{*2}}{1+sr^{*2}} + K\lambda_i)\lambda \\ + \frac{(g+\gamma_n s)\gamma' r^{*2}}{1+sr^{*2}} + K\lambda_i(\gamma_n + \frac{gr^{*2}}{1+sr^{*2}}) = 0 \end{array} \tag{30}$$

Similar to the arguments in the decoupled laser case, the following inequalities are equivalent to the claim that the real parts of the roots to (30) are negative:

$$\begin{array}{c} \gamma_n + \dfrac{(g+s\gamma')r^{*2}}{1+sr^{*2}} + K\lambda_i > 0 \\ \dfrac{(g+\gamma_n s)\gamma' r^{*2}}{1+sr^{*2}} + K\lambda_i(\gamma_n + \dfrac{gr^{*2}}{1+sr^{*2}}) > 0 \end{array} \tag{31}$$

Recall that the eigenvalues of L satisfies $\lambda_1 = 0, \lambda_i \geq 0$ for $2 \leq i \leq n$. For $i = 1$, $\lambda_1 = 0$ and the dynamic (28) is identical to the decoupled laser case (10) and the inequalities in (31) requires $0 < K < \gamma/2$ as $\gamma' = \gamma - 2K$, with positive system parameters $g, s, \alpha, \gamma, \gamma_n, N_0, J$. For $i = 2, 3, ...n$, $\lambda_i > 0$, so (31) clearly holds. ■

Theorem 2: Under Assumption 1, if each laser is operating around the limit cycle with the radius r^*, the carrier number N^* and the angular velocity $(-\alpha K + \omega)$, and the initial phase differences of lasers are small (*i.e.* $\Delta\theta'_k$ is around 0), the coupled laser system (1) locally asymptotically synchronizes to the same limit cycle for the coupling strength $0 < K < \gamma/2$.

Proof: We showed at the beginning of this section that the system (1) and its polar coordinate representation (3) can be linearized to (17) around the limit cycle $(r_k, N_k, \Delta\theta'_k) = (r^*, N^*, 0), \forall k$, under the condition that the decoupled laser is stabilized around it and the initial phase differences are small. We can see that the equilibrium of the system (17) indicates synchronization of the system (3), *i.e.*, $r_k \to r_j \to r^*, N_k \to N_j \to N^*, \theta_k \to \theta_j, \forall k, j$. From Lemma 1, we know that (17) is asymptotically stable, which then indicates synchronization as $t \to \infty$. ■

Remark 3: From Theorem 2, the coupling topology to guarantee synchronization is a general undirected connected graph. When the lasers are synchronized, *i.e.*, $E_k = E_j$ for all possible k and j, the dynamic of each laser in the coupled array becomes identical with each other and is also identical to the behavior of the decoupled laser dynamics shown in (5).

V. Simulation Examples

To illustrate the performance, we consider 5 coupled semiconductor lasers modeled by (1). The system parameters used are listed in the Table I, where the values are from a realistic experimental situation [18], [20].

TABLE I

Laser parameters that represent a realistic experiment.

Symbol	Description	Value
α	Linewidth enhancement factor	10^{-4}
γ	Photon decay rate	$500ns^{-1}$
γ_n	Carrier decay rate	$0.5ns^{-1}$
g	Differential gain coefficient	$1.5 \times 10^{-5}ns^{-1}$
N_0	Carrier numbers at transparency	1.5×10^8
s	Gain saturation coefficient	2×10^{-7}

Substitute these parameters into Eq. (7) and (11), and choose $\omega = 2$, coupling strength $K = 1 < \gamma/2$. We have the periodic solution of each decoupled laser is $(r^*, N^*) = (302.2562, 1.8381 \times 10^8)$ with angular velocity $\dot{\theta}^* = 1.0001$, and

$$A = \left[\begin{array}{cc} -8.9361 & 0.0022 \\ -2.9565 \times 10^5 & -1.8458 \end{array}\right] \tag{32}$$

The eigenvalues of A are $\lambda_1 = -5.3909 + 25.4089i$, $\lambda_2 = -5.3909 - 25.4089i$. According to Theorem 1, each decoupled laser system is stabilized on its periodic solution. In the presence of coupling, we simulate the case of all-to-all coupling and use the same parameters $\alpha, N_0, s, \gamma, \gamma_n, g$ and coupling strength K. According to Theorem 2, the coupled semiconductor system will locally synchronize asymptotically. Fig. 2 demonstrate the synchronization process of the system modeled by (17), which illustrates that $E_k(t) \to E_j(t),\ \forall k, j = 1, \ldots, n$, as $t \to \infty$. In the case of general coupling topology, we choose the coupling for the 5 laser array as shown in Fig. 3. Its synchronization process is shown in Fig. 4. We can see that the convergence time is longer than the all-to-all coupling case.

VI. Conclusion

In this paper, we considered coupled semi-conductor lasers modeled by nonlinear Lang and Kobayashi equations. We assume the coupling topology is modeled by an undirected connected graph with equal in-degrees. We first proved that the decoupled laser system is locally stabilized to a limit cycle under certain conditions on system parameters. Then, utilizing graph and systems theory, we rigorously proved that the coupled laser system locally synchronizes to the limit cycle. Simulations demonstrate the synchronization behaviors of 5 lasers in a generally connected topology. Future research includes considering time-delays and real experimental requirements.

References

[1] H. G. Winful and S. S. Wang. Stability of phase locking in coupled semiconductor laser arrays. *Appl. Phys. Lett.*, 53:1894–1896, 1988.

[2] S. S. Wang and H. G. Winful. Dynamics of phase locked semiconductor laser arrays. *Appl. Phys. Lett.*, 52:1774–1776, 1988.

[3] G. Kozyreff, A.G. Vladimirov, and P. Mandel. Global coupling with time delay in an array of semiconductor lasers. *Physical Review Letters*, 85:3809–3812, 2000.

[4] G. Kozyreff, A.G. Vladimirov, and P. Mandel. Dynamics of a semiconductor laser array with delayed global coupling. *Phys. Rev. E*, 64:016613, 2001.

[5] R. Lang and K. Kobayashi. External optical feedback effects on semiconductor injection laser properties. *IEEE Journal of Quantum Electronics*, 16(3):347–355, 1980.

[6] Y. Kuramoto. *Chemical Oscillations, Waves and Turbulence*. Springer-Verlag, Berlin, 1984.

[7] D. Botez and D. R. Scifres. *Diode Laser Arrays*. Cambridge University Press, Cambridge, England, 1994.

[8] Y. Braiman, T. A. B. Kennedy, K. Wiesenfeld, and A. Khibnik. Entrainment of solid-state laser arrays. *Physical Review A*, 52(2):1500–1506, 1995.

[9] L. Fabiny, P. Colet, R. Roy, and D. Lenstra. Coherence and phase dynamics of spatially coupled solid-state lasers. *Physical Review A*, 47(5):4287–4296, 1993.

[10] J. Garcia-Ojalvo, J. Casademont, M. C. Torrent, C. R. Mirasso, and J. M. Sancho. Coherence and synchronization in diode-laser arrays with delayed global coupling. *Int. J. Bif.*, 9(11):2225–2229, 1999.

[11] A. Hohl, A. Gavrielides, T. Erneux, and V. Kovanis. Localized synchronization in two nonidentical coupled lasers. *International Journal of Bifurcation and Chaos*, 23(25):4745–4748, 1997.

[12] A. Hohl, A. Gavrielides, T. Erneux, and V. Kovanis. Quasiperiodic synchronization for two delay-coupled semiconductor lasers. *Physical Review A*, 59(5):3941–3949, 1999.

[13] A. T. Winfree. *Geometry of Biological Time*. Springer-Verlag, New York, 1980.

[14] F. Ruiz-Oliveras, M. C. Soriano, P. Colet, and C. R. Mirasso. Information encoding and decoding using unidirectionally coupled chaotic semiconductor lasers subject to filtered optical feedback. *IEEE Journal of Quantum Electronics*, 45:962–968, 2009.

[15] I.V. Ermakov, V. Z. Tronciu, P. Colet, and C. Mirasso. Controlling the unstable emission of a semiconductor laser subject to conventional optical feedback with a filtered feedback branch. *Optics Express*, 17:8749–8755, 2009.

[16] A. Jacobo, M. C. Soriano, C. R. Mirasso, and P. Colet. Chaos-based optical communications: Encryption vs. nonlinear filtering. *IEEE Journal of Quantum Electronics*, 46(4):499–505, 2010.

[17] R. A. Oliva and S. H. Strogatz. Dynamics of a large array of globally coupled lasers with distributed frequencies. *International Journal of Bifurcation and Chaos*, 11(9):2359–2374, 2001.

[18] B. Liu, Y. Liu, and Y. Braiman. Coherent addition of high power laser diode array with a v-shape external talbot cavity. *Optics Express*, 16(25):20935–20942, 2008.

[19] C. D. Meyer, editor. *Matrix Analysis and Applied Linear Algebra*. Society for Industrial and Applied Mathematics, Philadelphia, PA, USA, 2000.

[20] B. Liu, Y. Braiman, Y. Lu, Y. Guo, P. Colet, and M. Wardlaw. Nonlinear dynamics and synchronization of an array of single mode laser diodes in external cavity subject to current modulation. *Optics Express*, 2012. submitted.

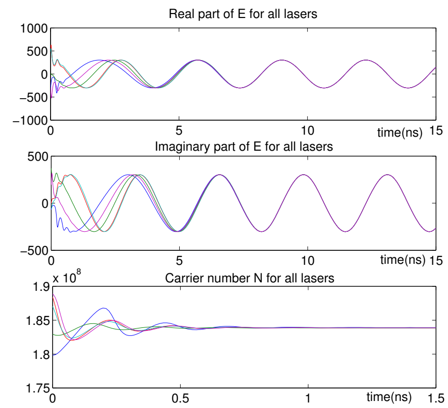

Fig. 2. Time history of state variables in the case of all-to-all coupling topology.

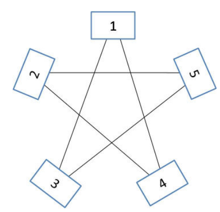

Fig. 3. The coupling topology.

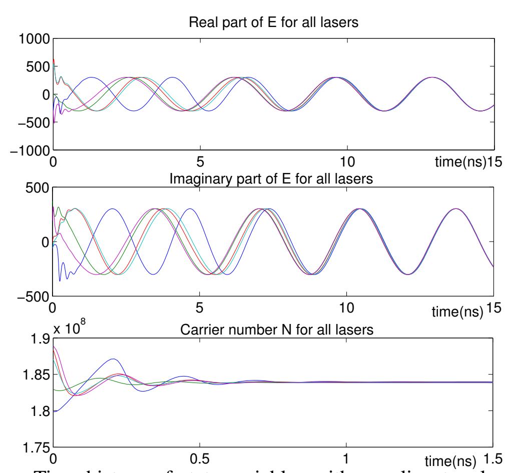

Fig. 4. Time history of state variables with coupling topology shown in Fig. 3.